$0.045\ \lambda_0 \times 0.16\ \lambda_0$, where λ_0 is the wavelength in free space at the operating frequency, for example, 2.35 GHz. As shown in Figure 5, the measurements agree well with the circuit and full wave simulations. The insertion loss is less than or equal to 1 dB in the band of 2.32–2.4 GHz (minimum: 0.96 dB at 2.36 GHz), which includes the loss caused by the microstip-SICL transitions and the 2.4–2.4 connectors that are used for the measurement. The out-of-band spurious response is below -27 dB until 13.68 GHz ($5.82f_0$). It can be seen that the second harmonic is suppressed successfully as predicted.

4. CONCLUSION

This article presents a BPF with extended rejection bandwidth based on SICL. A partial coupling scheme has been introduced for eliminating the harmonics, and the SICL technology ensures that the entire filter is arranged in a compact size. The experiments confirm that the proposed filter has merits of low loss, low crosstalk, easy integration, and a stopband up to $5.82f_0$, and it is a promising building block for high density integrated RF circuits.

ACKNOWLEDGMENT

This work was supported in part by National 973 project 2010CB327400 of China and National Science Foundation of Jiangsu province under Grant SBK201241785.

REFERENCES

1. C.-Y. Chang and T. Itoh, A modified parallel-coupled filter structure that improves the upper stopband rejection and response symmetry, IEEE Trans Microwave Theory Tech 39 (1991), 310–314.
2. I.J. Bahl, Capacitively compensated high performance parallel coupled microstrip filter, In: IEEE MTT-S International Microwave Symposium Digest, Long Beach, CA, 1989, pp. 679–682.
3. D. Ahn, J.S. Park, C.S. Kim, J. Kim, Y.X. Qian, and T. Itoh, A design of the low-pass filter using the novel microstrip defected ground structure, IEEE Trans Microwave Theory Tech 49 (2011), 86–93.
4. Y.X. Qian and T. Itoh, Planar periodic structures for microwave and millimeter wave circuit applications, In: IEEE MTT-S International Microwave Symposium Digest, Vol. 4, Anaheim, CA, 1999, pp. 1533–1536.
5. S.C. Lin, Y.S. Lin, and C.H. Chen, Extended-stopband bandpass filter using both half-and quarter-wavelength resonators, IEEE Microwave Wireless Compon Lett 16 (2006), 43–45.
6. Y.C. Li, X.Y. Zhang, and Q. Xue, Bandpass filter using discriminating coupling for extended out-of-band suppression, IEEE Microwave Wireless Compon Lett 20 (2010), 369–371.
7. Y. Mu, Z.W. Ma, and D. Xu, A novel compact interdigital bandpass filter using multilayer cross-coupled folded quarter-wavelength resonators, IEEE Microwave Wireless Compon Lett 15 (2005), 847–849.
8. M. Nosrati and M. Mirzaee, Compact wideband microstrip bandpass filter using quasi-spiral loaded multiple-mode resonator, IEEE Microwave Wireless Compon Lett 20 (2010), 607–609.
9. F. Gatti, M. Bozzi, L. Perregrini, K. Wu, and R.G. Bosision, A novel substrate integrated coaxial line for wide-band applications, In Proceedings of the 36th European Microwave Conference, Manchester, UK, September 2006, pp. 1614–1617.
10. P. Chu, W. Hong, K. Wu, et al., A miniaturized bandpass filter implemented with substrate integrated coaxial line, Microwave Opt Technol Lett 55 (2013), 131–133.
11. J.S. Hong and M.J. Lancaster, Microstrip filters for RF/microwave application, Wiley, New York, 2001.

© 2014 Wiley Periodicals, Inc.

BANDWIDTH IMPROVEMENT OF REFLECTARRAYS USING SINGLE-LAYERED DOUBLE CONCENTRIC CIRCULAR RING ELEMENTS ON A SUBWAVELENGTH GRID

Lu Guo, Peng-Khiang Tan, and Tan-Huat Chio
Temasek Laboratories, National University of Singapore, T-Lab Building, 5A, Engineering Drive 1, Singapore 117411; Corresponding author: tslguol@nus.edu.sg

Received 17 June 2013

ABSTRACT: *This article proposes the use of double concentric circular ring elements arranged in a subwavelength grid on a single layer of substrate, in an effort to increase the bandwidth of reflectarrays. Compared to the traditional $\lambda/2$ grid arrangements, radiating elements arranged in subwavelength grids achieves a more similar behavior over wider frequency bands when radiating elements' parameters are varied; albeit with a smaller reflected phase range. Furthermore, in contrast to conventional subwavelength single-patch designs that have only one variable parameter of the phasing element, the double concentric circular ring elements also allow additional degrees-of-freedom to improve the bandwidth. Based on the concentric ring element, two offset-fed 0.43 $\times$ 0.43 m^2 reflectarrays, one with $\lambda/2$ grid and another with $\lambda/3$ grid, centered at 10 GHz are designed and developed. The measured results show that the 2-dB gain bandwidth of the one with $\lambda/2$ grid spacing is 13.6%, whereas the one with $\lambda/3$ grid spacing is 24.4%.* © 2014 Wiley Periodicals, Inc. Microwave Opt Technol Lett 56:418–421, 2014; View this article online at wileyonlinelibrary.com. DOI 10.1002/mop.28111

Key words: *reflectarray; broadband; pyramidal horn; double circular ring element; subwavelength*

1. INTRODUCTION

Compared to parabolic dishes, reflectarrays have advantages of low profile and ease of fabrication. However, one major drawback of reflectarrays is their narrowband performance [1–3]. Various techniques have been proposed to improve the bandwidth of reflectarrays, such as multilayer designs [4, 5], single-layer multiresonant designs [6, 7], and aperture coupled designs [8, 9]. A different approach for broadband design has been introduced by using subwavelength elements instead of the conventional $\lambda/2$ elements [10–12]. It is demonstrated that the reflectarrays designed with subwavelength elements achieve a notable improvement in gain bandwidth performance. Nevertheless, to the authors' best knowledge, all the subwavelength element designs in the literatures so far are based on either single-layer [10, 11] or double-layer [12] single-patch geometries. No research has been done on subwavelength single-layer multiresonant elements, such as in the form of double concentric circular rings. By deploying single-layer multiresonant elements with subwavelength grid spacing, one could benefit from both the simple structure and improved bandwidth performance.

In this article, the feasibility of designing a broadband reflectarray using single-layer subwavelength double concentric circular ring elements is investigated. Numerical studies are undertaken to understand the broadband mechanism of single-layer subwavelength multiresonant elements. Based on these studies, two offset-fed X-band reflectarrays are designed and developed using variable sized double concentric circular rings. One is designed with traditional $\lambda/2$ grids and the other one with $\lambda/3$ grids. Although both reflectarrays feature relatively good performance, the one designed with closely spaced

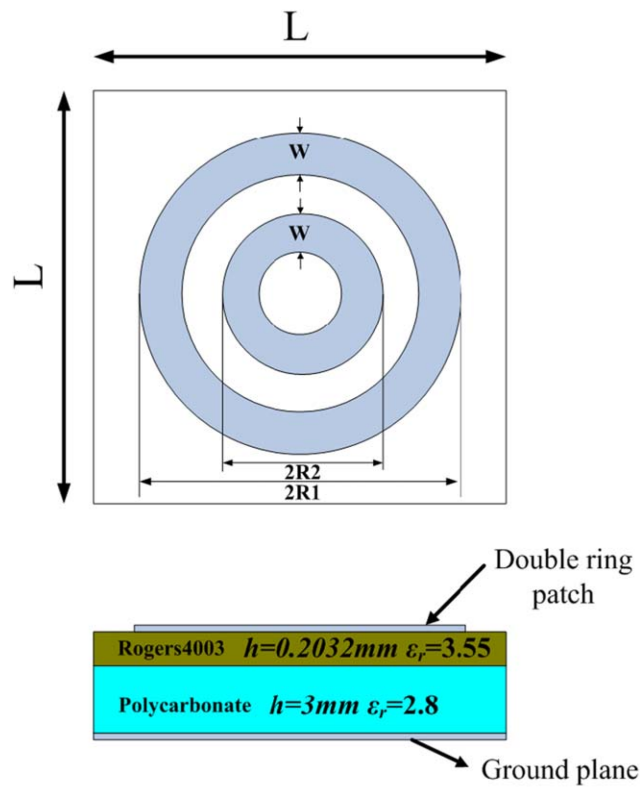

Figure 1 Geometry of the double concentric ring element. [Color figure can be viewed in the online issue, which is available at wileyonlinelibrary.com]

elements demonstrates a 10.8% increase in the 2-dB gain bandwidth.

2. ELEMENT DESIGN AND PERFORMANCE

In this study, a multiresonant element in the form of variable sized double concentric circular rings is used. This is similar to the one in Ref. [6] where a relatively small 81-element single-layered reflectarray is built. Although [6] shows a good bandwidth performance, the performance in a large array is not reported. This work deploys the elements in a much larger array of 1640 elements in a 0.43×0.43 m^2 aperture with $\lambda/3$ grid spacing.

Figure 1 depicts the basic configuration of the element design. The double concentric circular ring elements are printed on a Rogers 4003 substrate with thickness of 8 mil, dielectric constant of 3.55, and loss tangent of 0.0027, supported by a layer of 3-mm polycarbonate ($\varepsilon_r = 2.8$) and backed by a conducting ground plane. The element geometry offers an increased span of phase variation compared to the single-circular ring, whereas the polycarbonate layer provides the necessary thickness for a slow varying phase variation when the double-ring dimensions are changed. This is essential to obtain wideband performance. The design operates at X-band centered at 10 GHz. The reflectarray is assumed to be formed by identical elements arranged in square lattices. Phase characteristics with two grid spacings, that is, $\lambda/2$ and $\lambda/3$, are investigated to understand the broadband mechanism of single-layer subwavelength double concentric circular ring elements. The reflection phase curves can be obtained by considering an infinite array of identical elements with a plane wave incidence upon them [13].

Figure 2 plots the reflected phase response versus outer ring radius $R1$ with grid spacing $L = 15$ mm ($\lambda/2$), at 9, 10, and 11 GHz, respectively. Other parameters are set as optimal, that is, $w = 0.08 \times R1$ and $R2 = 0.8 \times R1$. It is noticed in Figure 2 that the double concentric ring element features a span of phase change in excess of 600°. The slope of the phase variation is relatively gentle.

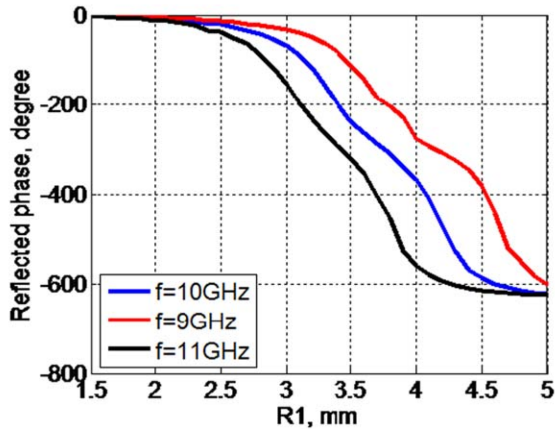

Figure 2 Reflected phase curves of the double concentric circular ring element with grid spacing of $\lambda/2$ (15 mm) for different frequencies. [Color figure can be viewed in the online issue, which is available at wileyonlinelibrary.com]

Figure 3 is the same as Figure 2 except that the grid spacing is $L = 10$ mm ($\lambda/3$). Other parameters remain the same, that is, $w = 0.08 \times R1$ and $R2 = 0.8 \times R1$.

Comparing Figure 2 with Figure 3, it is shown that the reflected phase curves are less linear and more sensitive to the frequency variation when the grid spacing is $\lambda/3$. Therefore, the bandwidth is not expected to be improved.

In order to linearize the phase curves and make them less sensitive to the frequency variation, the spacing between the double circular rings needs to be optimized when applied in a subwavelength grid. Herewith is the advantage of the double concentric ring element. For single-patch elements such as proposed in Refs. [10] and [11], there is only one variable parameter of the phasing element, that is, the patch length. For the double concentric ring elements proposed here, additional parameters can be varied as well, such as the spacing between

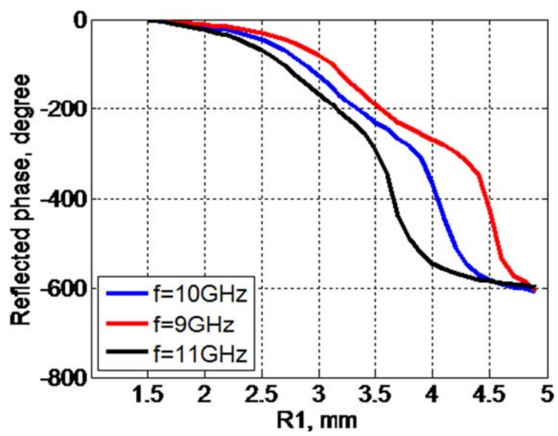

Figure 3 Reflected phase curves of the double concentric circular ring element with grid spacing of $\lambda/3$ (10 mm) and relation of $w = 0.08 \times R1$, $R2 = 0.8 \times R1$ for different frequencies. [Color figure can be viewed in the online issue, which is available at wileyonlinelibrary.com]

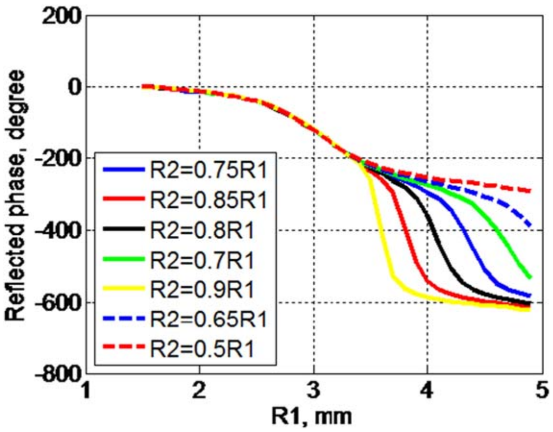

Figure 4 Reflected phase curves with different ring spacings at 10 GHz. [Color figure can be viewed in the online issue, which is available at wileyonlinelibrary.com]

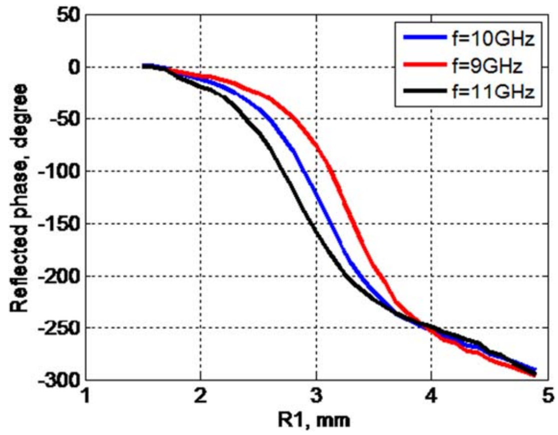

Figure 5 Reflected phase curves of the double concentric circular ring element with ring spacing of $R2 = 0.5R1$ for different frequencies. [Color figure can be viewed in the online issue, which is available at wileyonlinelibrary.com]

the double rings. Those parameters are optimized to achieve a good performance in a $\lambda/3$ grid spacing. Figure 4 illustrates the reflected phase curves with different double ring spacings at 10 GHz. It is observed that the spacing between the two rings affects the linearity of the phase curves quite significantly. With the increase of the ring spacing, phase curves are more linear but at the expense of the phase range. It is found that the curve of $R2 = 0.5R1$ shows good linearity while offering a sufficient phase range. Therefore, the double circular ring spacing is chosen as $R2 = 0.5R1$.

Figure 5 depicts the reflected phasing curves of the double concentric circular ring element with ring spacing of $R2 = 0.5R1$ for different frequencies. It is noticed that the phase curves feature more linear behavior and less sensitive to the frequency variation. Therefore, a broadband performance is expected to be obtained.

3. IMPLEMENTATION AND PERFORMANCE OF THE REFLECTARRAYS

In this work, a pyramidal horn antenna is designed and manufactured to illuminate the reflectarray. The critical parameters of the pyramidal horn are optimized by HFSS to achieve the desired behavior at the operational band. A 10-dB edge illumination of the reflectarray is assumed and an offset feed method is adopted to avoid aperture blockage. Two X-band reflectarrays are designed and fabricated for the operating frequency of 10 GHz. One is designed using the traditional $\lambda/2$ grid spacing and the other one is designed with $\lambda/3$ grid spacing while the spacing of the double concentric ring element is chosen to be $R2 = 0.5R1$. For the comparison purpose, another reflectarray using $\lambda/3$ grid but with the ring spacing of $R2 = 0.8R1$ is also built to gain some insights into the broadband mechanism of single-layer subwavelength multiresonant elements. All antennas have a square aperture of 430×430 mm^2 hosting 729 and 1640 elements for $\lambda/2$ and $\lambda/3$ arrays, respectively. In this study, the elements' reflection phases are designed to generate a beam in the direction of $(\theta_b, \varphi_b) = (25°, 0°)$. Prototypes of the reflectarrays are shown in Figure 6.

Figure 7 presents the measured radiation patterns of three reflectarrays at 10 GHz. It is seen that the peak gain occurs at 25° off-broadside in all three reflectarrays. The measured side lobe level is below 15 dB in both principal planes for all reflectarrays and at the region around the main lobe, the cross polarization level is about 30 dB.

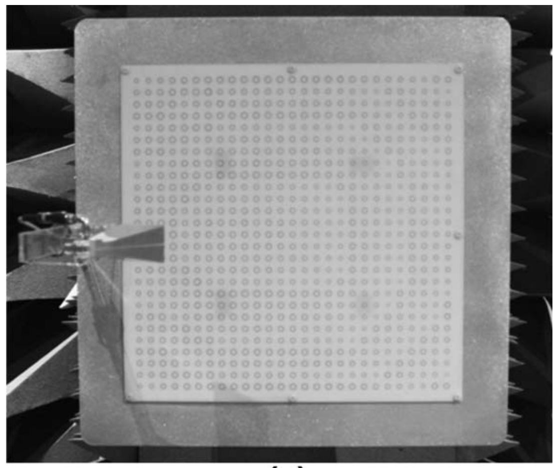

(a)

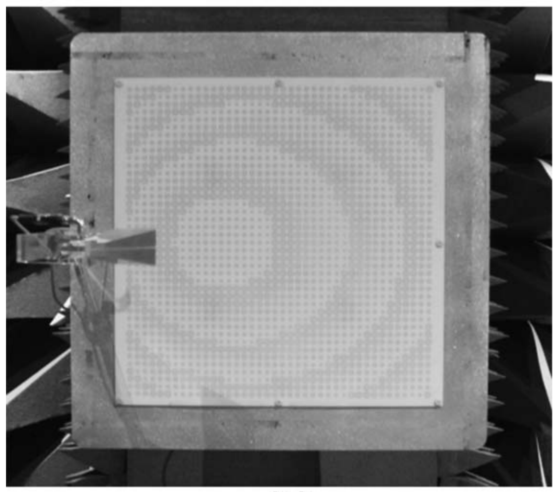

(b)

Figure 6 Prototypes of the reflectarrays. (a) $\lambda/2$ array with 729 double concentric circular rings and (b) $\lambda/3$ array with 1640 double concentric circular rings with the ring spacing of $R2 = 0.5R1$

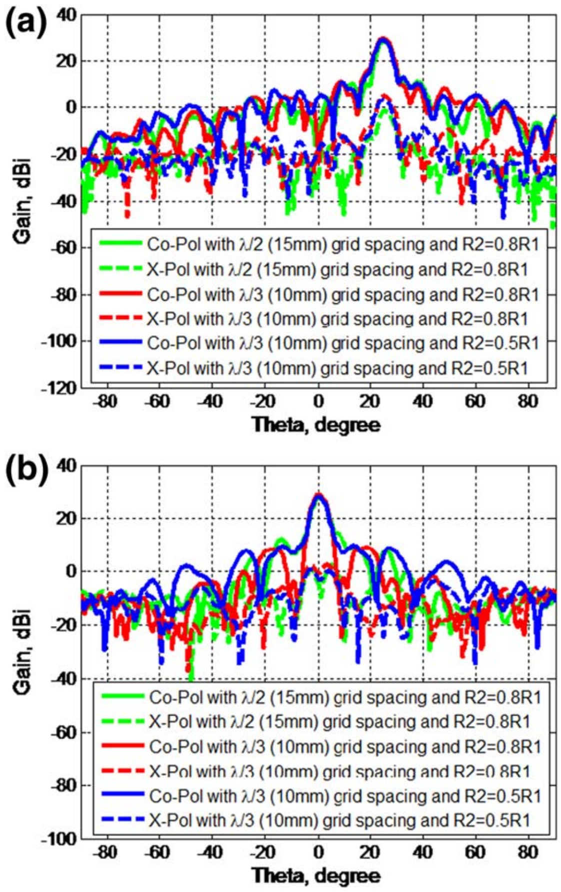

Figure 7 Measured gain radiation patterns in principal planes at 10 GHz for three reflectarrays. (a) *x-z* plane and (b) on the plane forming an angle of 25° with *y-z* plane. [Color figure can be viewed in the online issue, which is available at wileyonlinelibrary.com]

The measured gain performance of reflectarrays is displayed in Figure 8. The measured maximum gains of the reflectarrays are 28.5 and 29.17 dBi for $\lambda/2$ array and $\lambda/3$ array with ring spacing of $R2 = 0.5R1$, which correspond to an aperture efficiency of 34.12 and 39.82%, respectively. Note that although $\lambda/3$ array with ring spacing of $R2 = 0.8R1$ shows a slightly higher maximum gain, the gain drops dramatically from 10.2 GHz onwards, as seen in Figure 8. This reflects the results in Section 2 where the reflected phase curves of elements with ring spacing of $R2 = 0.8R1$ exhibit less linear behavior and more sensitive to the frequency variation, therefore, leading to a less wideband behavior. The measured results also show that the $\lambda/3$ array with ring spacing of $R2 = 0.5R1$ achieves a significant bandwidth improvement compared to the $\lambda/2$ array, where the 2-dB gain bandwidth has been increased from 13.6 to 24.4%.

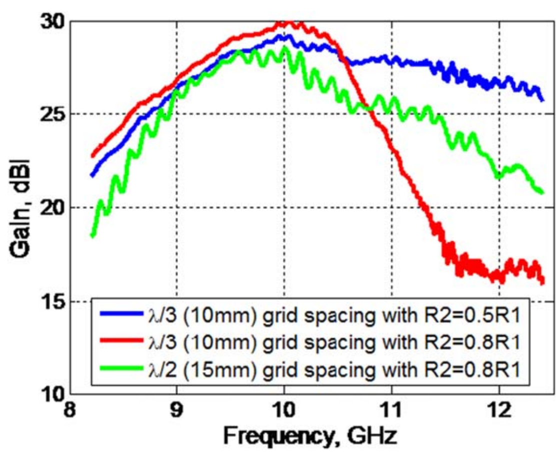

Figure 8 Measured gain of the reflectarrays. [Color figure can be viewed in the online issue, which is available at wileyonlinelibrary.com]

4. CONCLUSION

The concept of using single-layer subwavelength double concentric circular ring elements for reflectarray bandwidth improvement has been studied both numerically and experimentally. Numerical investigations are conducted to understand the broadband mechanism of single-layer subwavelength multiresonant elements. As an alternative to the traditional subwavelength single-patch designs that have only one variable parameter of the phasing element, additional parameters of the double concentric circular ring element such as the spacing between the two rings are varied to achieve a good performance when applied on a $\lambda/3$ grid. The measured results show a considerable bandwidth improvement, where the 2-dB gain bandwidth has been increased from 13.6 to 24.4%.

REFERENCES

1. J. Huang and J.A. Encinar, Reflectarray antennas, Institute of Electrical and Electronics Engineers, Wiley, Hoboken, NJ, 2008.
2. Q.Y. Li, Y.C. Jiao, and G. Zhao, A novel microstrip rectangular-patch/ring combination reflectarray element and its application, IEEE Antennas Wireless Propag Lett 8 (2009), 1119–1122.
3. R.H. Li, L. Chen, X.T. Gu, and X.W. Shi, A novel element for broadband reflectarray antennas, J Electromagn Waves Appl 25 (2011), 1554–1563.
4. J.A. Encinar and J.A. Zomaza, Broadband design of three-layer printed reflectarrays, IEEE Trans Antennas Propag 51 (2003), 1662–1664.
5. J.A. Encinar, Design of two-layer printed reflectarrays using patches of variable size, IEEE Trans Antennas Propag 49 (2001), 1403–1410.
6. Y. Li, M.E. Biakowski, K.H. Sayidmarie, and N.V. Shuley, 81-element single-layer reflectarray with double-ring phasing elements for wideband applications, In: 2010 IEEE Antennas and Propagation Society International Symposium, July11–17, 2010, Toronto, Canada.
7. Y. Li, M.E. Biakowski, K.H. Sayidmarie, and N.V. Shuley, Single-layer microstrip reflectarray with double elliptical ring elements for bandwidth enhancement, Microwave Opt Technol Lett 53 (2011), 1083–1087.
8. A.W. Robinson, M.E. Bialkowski, and H.J. Song, A passive reflect-array with dual-feed microstrip patch elements, Microwave Opt Technol Lett 23 (1999), 295–299.
9. A.W. Robinson, M.E. Bialkowski, and H.J. Song, An 137-element active reflect-array with dual-feed microstrip patch elements, Microwave Opt Technol Lett 26 (2000), 147–151.
10. D.M. Pozar, Wideband reflectarrays using artificial impedance surfaces, Electron Lett 43 (2007), 148–149.
11. P. Nayeri, F. Yang, and A.Z. Elsherbeni, Bandwidth improvement of reflectarray antennas using closely spaced elements, Prog Electromagn Res C 18 (2011), 19–29.
12. P. Nayeri, F. Yang, and A.Z. Elsherbeni, Broadband reflectarray antennas using double-layer sub-wavelength patch elements, IEEE Antennas Wireless Propag Lett 9 (2010), 1139–1142.
13. D.M. Pozar, S.D. Targonski, and H.D. Syrigos, Design of millimetre wave microstrip reflectarrays, IEEE Trans Antennas Propag 45 (1997), 287–296.

© 2014 Wiley Periodicals, Inc.